Institut für Physikalische Elektronik

Institute of Physical Electronics

Universität Stuttgart

Jahresbericht

Annual Report 2010

Jahresbericht
Annual Report

2010

Redaktion • edited by:

Jürgen Köhler
Jürgen H. Werner
Leo Bauer
grafik-service@web.de

Vorwort

Liebe Freunde des *ipe*,

dieser Jahresbericht legt wieder einen Ausschnitt unserer Aktivitäten in Forschung und Lehre dar. Zwei neue Forschungsbereiche sind in den letzten Jahren am *ipe* entstanden: i) der Einsatz von Lasern bei immer mehr Prozessen in der Herstellung von Solarzellen und ii) die Analyse und Entwicklung von Alternativen zu Giftstoffen in Photovoltaikmodulen. Diese Arbeiten werden wir in den nächsten Jahren verstärkt fortsetzen. Ferner richtet sich unser Augenmerk immer mehr auf das gesamte Photovoltaikmodul und auf Anlagen als auf die Optimierung der Eigenschaften von einzelnen Zellen.

Es ist absehbar, dass es in den nächsten Jahren zu einer Marktbereinigung unter den Anbietern von Zellen, Modulen und Anlagen kommen wird. Umso mehr ist es für uns wichtig, nicht nur mit kompetenten, starken Industriepartnern zusammen zu arbeiten, sondern ihnen auch immer wieder originäre und originelle Forschungsergebnisse anbieten zu können. Nur so kann heute ein Universitätsinstitut in der angewandten Photovoltaikforschung überleben. Auch die Lehre wird mit noch mehr Spezialvorlesungen zur Photovoltaik weiter ausgebaut, denn auf nicht absehbare Zeit besteht in der Photovoltaik-Industrie und ihren Zulieferern ein riesiger Bedarf an kompetenten Naturwissenschaftlern und Ingenieuren.

Ich danke allen Mitgliedern des *ipe* für die tolle Arbeit im Jahr 2010.

Stuttgart, Dezember 2010

Jürgen H. Werner

Preface

Dear friends of *ipe*,

this annual report presents some of our teaching and research activities in 2010. Within the last few years, we developed two new research fields: i) laser processes in the fabrication of solar cells, and ii) the analysis and the development of alternatives for toxic materials in photovoltaic modules. Within the next few years we will even strengthen these activities. Also, our focus will move more to the design and optimization of photovoltaic modules and systems, instead of mainly concentrating on cell technologies.

It is easy to foresee, that photovoltaics will face a shakeout in the number of companies producing cells, modules, and/or systems. Only large (and fully integrated) or highly specialized companies will probably survive the strong competition. Thus, it is essential for us, not only to cooperate with strong industrial partners, but also to offer them even more innovative and original research results. In addition, we will extend our teaching activities by offering more specialized lectures in the field of photovoltaics. The market is still demanding more and more engineers and scientists with a high expertise in photovoltaic technologies.

I am grateful for and proud of the excellent work of all members of *ipe* in 2010.

Stuttgart, December 2010

J. Werner

Jürgen H. Werner


Institut für Physikalische Elektronik

Inhaltsverzeichnis • Table of Contents

Mitarbeiter
People

Dünnschichttechnik

Solarzellen

Mikro - und Optoelektronik

Weltrekord

Institutsleitung • Head of the Institute

Verwaltung • Administration

Gruppe Laserprozesse
Group Laser Processing

(Gruppenleiter / Group Leader: Jürgen Köhler)

Die Gruppe „Laserprozesse“ entwickelt neue Technologien zur Laserprozessierung einkristalliner und multikristalliner Silizium-Scheiben. Hierzu zählen die laserunterstützte Abscheidung von Metallkontakten, die Kantenisolierung von Solarzellen sowie die Laserdotierung zur Herstellung von ganzflächigen und selektiven Emittern für kristalline Silizium-Solarzellen. Im Vordergrund unserer Arbeiten stehen Grundlagenuntersuchungen zur Laserdotierung sowie zur laserunterstützten Feinlinienmetallisierung, Entwicklungsziele sind die Erhöhung des Durchsatzes bei der laserunterstützten Emitterdotierung sowie die Steigerung der Wirkungsgrade von bis zu 156 mm x 156 mm großen einkristallinen und multikristallinen Silizium-Solarzellen auf über 18%. In enger Zusammenarbeit mit der Gruppe „Industrielle Solarzellen“ am *ipe* optimieren wir unseren Laserdotierprozess für selektive Emitter zusammen mit der Siebdrucktechnik.

The “Laser Processing“ group explores new technologies for laser processing of mono- and multi-crystalline silicon wafers. Examples are laser assisted metal deposition, laser edge isolation as well as laser doping for full area and selective emitters of crystalline silicon solar cells. The main topic of our research work is the investigation of the fundamental processes involved in pulsed laser doping as well as in laser assisted fine line metallization. Development goals are the increase of the throughput rate of the laser doping process as well as the increase of the efficiency of up to 156 mm x 156 mm sized mono- and multi-crystalline silicon solar cells to more than 18%. A close collaboration with the “industrial solar cells“ group at *ipe* optimizes our selective emitter laser doping process together with screen printing technology.

Gruppe Technologie
Group Technology

(Gruppenleiterin / Group Leader: Birgitt Winter)

Die Gruppe „Technologie“ setzt sich aus den technischen Mitarbeitern des gesamten Instituts zusammen. Damit sind verschiedene Aufgabenstellungen zur Absicherung der Institutsinfrastruktur, zu Prozessen und Prozessschritten sowie zu Routinemesstechniken zusammengefasst. Diese Vernetzung im technischen Bereich ermöglicht eine gute Koordinierung aller anfallenden Arbeiten, sei es bei Routineanalysen, Messplatzerweiterungen, Laborumbaumaßnahmen oder auch bei der Weiterentwicklung wichtiger Technologien, wie Nasschemie, Lithographie, Metallisierung, Diffusion, Oxidation sowie diversen Plasmadepositionsverfahren und vieles andere mehr. Die Techniken sind immer wieder weiterzuentwickeln, verursacht durch neue Anforderungen, die aus laufenden Projekten erwachsen. Dabei ist die enge Zusammenarbeit bei Planung und Ergebnisdiskussion eine gute Grundlage mit dem Ziel, die Reproduzierbarkeit der Prozesse und Abläufe durch die Entwicklung von Qualitätskontrollstandards und standardisierten Prozessabläufen zu gewährleisten.

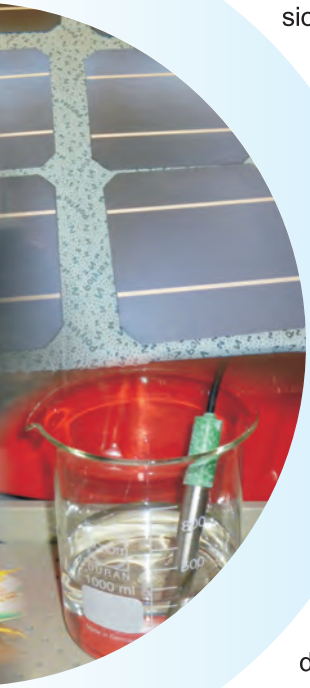

The group “Technology” pools all technical assistants and engineers. We support the laboratory infrastructure, perform the different standard processes and do routine measurements. The cross linking of technical experience allows an effective coordination of the requested demands. We make standard analyses, upgrade measurement setups, coordinate the reconstruction of the laboratory and enhance technical processes. We especially work on wet chemistry, metallization, lithography, diffusion and oxidation as well as on different plasma deposition methods etc. All techniques have to be adapted and developed in direction of requirements of the current scientific projects at *ipe*. Our goal is a high reproducibility of all process steps as described above by developing quality control requirement and standard procedures.
A close teamwork on planning and discussion of the results is seen as a proper base.

Gruppe Neue Materialien
Group New Materials

(Gruppenleiter / Group Leader: Gerhard Bilger)

Die Gruppe „Neue Materialien“ befasst sich mit der Entwicklung von neuartigen Materialien als passive Beschichtung von Solarzellen der dritten Generation, um mit diesen erhöhte Wirkungsgrade erzielen zu können. Mit dem Verfahren der Hochfrequenz-Zerstäubung (HF-Sputtern) lassen sich dünne Schichten aus praktisch allen Elementen des Periodensystems herstellen, wobei auch reaktive Gase die Schichtzusammensetzung beeinflussen können. Die Abscheidung von Dotierschichten als Prekursoren für die Dotierung von Si-Solarzellen mit Niedertemperatur-Laserprozessen verwendet ebenfalls dieses Sputter-Verfahren. Für die notwendige Charakterisierung dieser Schichten und der Dotiergradienten findet die Sekundärionen-Massenspektrometrie (SIMS) sowie die Röntgen- und Ultraviolett-Photoelektronen-Spektrometrie (XPS, UPS) Anwendung. Die Oberflächenanalytik unterstützt auch wesentlich alle Forschungs- und Entwicklungsgruppen am *ipe* und wird als Dienstleistung für andere Institute und die Industrie angeboten.

The group “New Materials“ develops novel materials as passive coatings on third generation solar cells to increase the quantum efficiency. These materials are processed as thin films by means of high frequency sputtering techniques which admit the preparation of layer compositions from nearly all elements of the periodic system including the addition of reactive gases. This sputtering technique is also applied for deposition of dopants as precursors for low-temperature laser processing in optimized Si solar cell doping. As methods to analyse these thin films and dopant profiles, the group uses secondary ion mass spectrometry (SIMS) as well as X-ray and ultraviolet photoelectron spectrometry (XPS, UPS). The surface analyses also substantially supports all research and development groups at the *ipe* and is offered to other institutes and industry.

Gruppe Dünnschichtsilizium
Group Thin Film Silicon

(Gruppenleiter / Group Leader: Markus Schubert)

Die Arbeitsgruppe „Dünnschichtsilizium“ des *ipe* entwickelt Solarzellen und Photodetektoren auf der Basis amorphen und nanokristallinen Siliziums. Flexible Photovoltaikmodule entstehen mit Hilfe der *in-situ* Serienverschaltung. Niedertemperaturprozesse nutzen ultradünne amorphe Siliziumschichten zur Passivierung und Verbesserung kristalliner Siliziumsolarzellen. In der photovoltaischen Systemtechnik vergleichen wir die Standorte Stuttgart, Nikosia und Kairo und untersuchen dabei den Einfluss von Material, Solarzellentyp und Klima auf den Jahresenergieertrag der netzgekoppelten Anlagen. Die dynamische elektronische Verschaltung verbessert die Energieausbeute von Photovoltaiksystemen. Spezielle Dünnschicht-Photodetektoren dienen der schnellen patientennahen Quantifizierung von Herzinfarkt-, Tumor- und Entzündungsmarkern in einem mobilen elektro-optischen Mikrosystem, welches wir in Zusammenarbeit mit mehreren Instituten der Universitäten Tübingen und Stuttgart sowie dem Institut für Mikroelektronik Stuttgart entwickeln.

The “Thin Film Silicon” group at *ipe* is developing solar cells and photodetectors based on amorphous and nanocrystalline silicon thin films. Flexible photovoltaic modules prove the novel in situ series connection technique. Low temperature processes deposit ultrathin amorphous silicon layers for passivating and improving crystalline silicon solar cells. Photovoltaic system technology compares the locations Stuttgart, Nicosia and Cairo, in order to investigate the effects of different materials, solar cell types, and climates on the annual energy yield of the grid-connected systems. Novel thin film photodetectors enable the quantification of e.g. heart attack, cancer, and inflammation markers in a mobile microsystem for so-called point-of-care testing which we develop in cooperation with several institutes of the universities Tübingen and Stuttgart, and with the Institut für Mikroelektronik Stuttgart.

Gruppe Industrielle Solarzellen
Group Industrial Solar Cells

(Gruppenleiterin / Group Leader: Renate Zapf-Gottwick)

Die Forschungsaktivitäten unserer Gruppe „Industrielle Solarzellen“ zielen auf industrienahe Prozesse, die den Wirkungsgrad von kristallinen Solarzellen verbessern. Wir optimieren gezielt an den einzelnen Schritten in der Herstellungskette einer Solarzelle: am Emitter, am Lichteinfang (an der Textur) und an den elektrischen Kontakten, die wir über Siebdruck aufbringen. Die Kontaktbildung ist beeinflusst durch die Kombination aus Sieb, Paste, verschiedenen Druckparametern und den Temperaturen beim Trocknen und Feuern. Vorderseitenkontaktgitter und vollflächige Metallisierung auf der Rückseite der Solarzelle werden auf geringe optische und elektrische Verluste optimiert. Zusammen mit der Gruppe „Laserprozesse“ am *ipe* integrieren wir die Laserprozesse, insbesondere die selektive Emittertechnologie, in die Prozessierung unserer Solarzellen.

Our group “Industrial Solar Cells” is engaged in different research activities gaining in higher efficiencies of solar cells by industry oriented processes. Our goal is to improve the different process steps in the production of solar cells: the emitter, light trapping (new textures) and the electrical contacts. Electrical contacts are fabricated by screen printing, the most common used technique in industry. Screen, paste, different print parameters and the temperatures of drying and firing influence the process of contact formation. The contact grid on the front side and the full area back contact are minimized in electrical and optical losses. Together with the group “laser processing“ at *ipe,* we integrate the laser doping process into the processing of our solar cells, especially the selective emitter technology.

Gruppe Charakterisierung
Group Device Analysis

(Gruppenleiter / Group Leader: Gerda Gläser, Michael Reuter)

Die Arbeitsgruppe „Charakterisierung“ beschäftigt sich mit der Analyse und Simulation der Eigenschaften von halbleitenden Schichten, Solarzellen und photovoltaischen Systemen. Dabei stehen der Gruppe Aufbauten zur elektrischen und optischen Messung der Lebensdauer, Strom/Spannungs-Charakteristik, Quantenausbeute, Elektro- und Photolumineszenz und ortsaufgelösten Kurzschlussstromdichte zur Verfügung. Die prozessbegleitende Charakterisierung kontrolliert und evaluiert die einzelnen Herstellungsschritte von Solarzellen aus mono- und multikristallinem Material. Ein weiterer Schwerpunkt ist die Entwicklung von innovativen Konzepten zur Wirkungsgradsteigerung von Solarzellen und -modulen. Streuzentren in bisher nur elektrisch aber nicht optisch aktiven Kontakten und Kontaktschichten zielen auf die bessere Einkopplung des Lichts in Solarzellen und Modulen.

Michael Reuter

The “Device Analysis“ group deals with the characterization and simulation of semiconductor layers, solar cells and photovoltaic systems. Thereby the group makes use of measurements setups for the electrical and optical device characterization, e.g. lifetime measurements, current/voltage-characteristics, quantum efficiency, electro- and photoluminescence and measurement of spatially resolved short circuit current density. The process accompanying characterization monitors and evaluates the production steps of mono- and multi-crystalline silicon solar cells. The group further develops novel concepts for photovoltaic efficiency enhancement. Scattering of light with so far only electrically active contacts and contact layers aims at the more efficient coupling of light into photovoltaic devices.

einkristallines

mikrokristallines

Silizium

nanokristallines

amorphes

Wissenschaftliche Beiträge
Scientific Contributions

Publikationen
Publications

Diffractive Laser Texture of ZnO:Al for Thin Film Photovoltaics

Author: M. Sämann

Efficient solar cells must completely absorb the solar spectrum. The optical absorption of solar cells, however, is wavelength dependent and decreases with increasing wavelength. Silicon thin film solar cells need textured electrodes to lengthen the light path inside their absorber layer, and thereby permit to reduce their thickness. For that purpose, micromorph tandem cells employ textured electrodes to cut the microcrystalline silicon thickness by half, and thereby save deposition time and cost. State-of-the-art textures, like Asahi® U-type glass [1], scatter short wavelength light, but fail for longer wavelengths.This contribution introduces a new approach to enhance light trapping by laser texturing the transparent aluminum doped zinc oxide (ZnO:Al) front contact. A line-focused pulsed ultraviolet laser scans and locally melts the ZnO:Al surface and thus creates a wave-like surface structure. Rotating the substrate by 90° and scanning again, produces a pyramid-like texture with an aspect ratio of 0.15. The periodic texture diffracts light and results in a haze factor (ratio of total to diffusive optical transmission) H > 90% in the visible range. Sheet resistances of $R_{\square} = 3\ \Omega/\square$ for $d = 2$ µm textured films comply with the demand of photovoltaic industries with $R_{\square} < 10\ \Omega/\square$.

Figures 1a and 1b show Scanning Electron Microscopy (SEM) images of laser textured ZnO:Al. Figure 1a presents the cross section of a 1 µm thick film after laser irradiation. Laser processing displaces material from the center of the pulse to its edges. The center film thickness decreases to 725 nm and increases by 10% at the edges. Figure 1b shows the surface with optimized pulse overlaps in x- and y-direction. The aspect ratio is 0.1 along the x- and y-axes, and 0.15 in the diagonal direction. Figure 2 shows total and diffusive transmittances of Asahi U-type glass compared to laser textured ZnO:Al. Asahi U-type glass only scatters short wavelength light, but fails for long wavelength light.

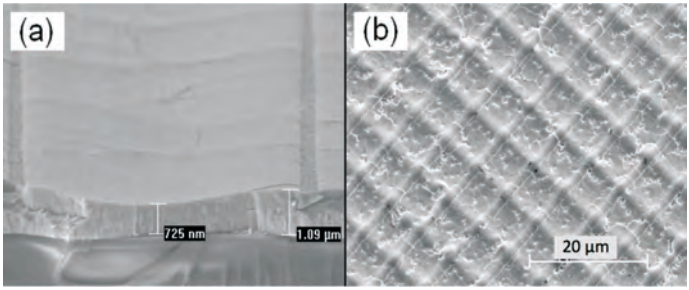

Figures 1:
SEM images. a) Cross section of a 1 µm thick ZnO:Al film after single laser pulse. Material is displaced from the center to the edges of the pulse, where an elevation piles up. b) Surface of laser textured ZnO:Al shows mountains and valleys.

Laser textured ZnO:Al achieves diffusive transmittances $T_{diff} > 70\%$ over the visible spectral range with a haze factor $H > 90\%$. The diffusive transmittance T is as high as $T > 30\%$ at $\lambda = 1000$ nm.

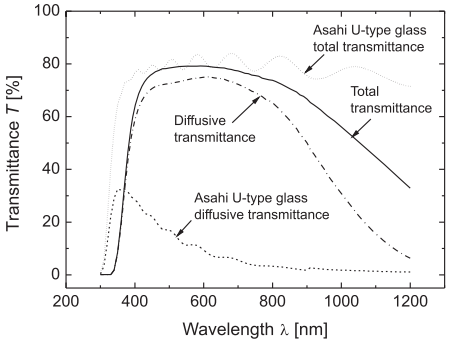

Figure 2:
Total and diffusive transmittance of Asahi U-type glass compared to laser textured ZnO:Al. Asahi U-type glass only scatters short wavelength light. Laser textured ZnO:Al shows a diffusive transmittance $T_{diff} > 70\%$ over the visible spectral range with a haze factor (ratio of diffusive to total transmittance) $H > 90\%$.

References:

[1] M. Mizuhashi, Y. Gotoh, K. Adachi, Jpn. J. Appl. Phys. **27**, 2053 (1988)

PV research plant at the University of Bahir Dar, Ethiopia

Authors: T. Klaus
In collaboration with: B. Zinßer, T. Wurster, A.-K. Müller,
A. Titos (centrotherm), J. Fröbel (Papendorf SE), and J. H. Werner

In September 2010, *ipe* researchers in collaboration with Ethiopian students and scientists set up a PV power plant at the Institute of Technology (IoT) at Bahir Dar University, Ethiopia. With a rated power of about 10 kW_p it is at present the largest PV system in Ethiopia. The project was conducted within the scope of a one week *Summer School on Photovoltaics*. This event marks the beginning of a long term cooperation of IoT and *ipe*.

The PV system is designed to fulfil several functions: First, it serves as a PV demonstration plant for students of "Renewable Energy" and related subjects. Secondly, it is fully equipped with sensors for research on PV at the IoT and other interested universities.

Figure 1:
Summer school team in front of the PV system

Thirdly, it contributes to a reliable power supply for the university campus, given the frequent power cuts lasting up to one day. Fourthly, the PV system functions as a University of Bahir Dar beacon project for the use of photovoltaics in Ethiopia. Thus, a flexible system was designed that is partly grid connected, partly functioning as an island-backup system in case of power cuts.

This project would not have been possible without the support of sponsors from the industry: centrotherm AG contributed half of the PV modules and the backup batteries. With their expertise and manpower they were a key factor for success. SolarWorld AG supported the project with the second half of the modules. Papendorf SE was responsible for design, provision, and setup of the measurement equipment. Important contributions came from Studer Innotec, Frank Zenkel, Peter Adelmann, as well as Rolf Gengenbach Messtechnik.

Figure 2:
A. Titos (centrotherm) with students after installing one of the inverters

Analysis of 100 µm thin String Ribbon Solar Cells

Author: P. Gedeon
In collaboration with: J. Cichoszewski, K. Carstens, J. H. Werner, and M. Reuter

Mono and multi-crystalline silicon wafers with a thickness d < 180 µm are technically challenging and uneconomic due to a high kerf loss that wastes 40 % to 60 % of the ingot material [1]. This restriction is not valid for String Ribbon (SR) wafers, which can be fabricated at virtually any thickness without any material loss due to sawing. We process untextured SR wafers with different mean thickness to solar cells. A mean thickness reduction from d = 180 µm to 100 µm leads to an efficiency loss $\Delta\eta$ = -0.6 %, a short circuit current density drop ΔJ_{SC} = -0.7 mAcm^{-2}, and an open circuit voltage drop ΔV_{OC} = -6 mV.

Figures 1a, b show a PC1D simulation calculating the expected η, J_{SC} and V_{OC} for wafer thicknesses varying from d = 200 µm down to d = 50 µm. The points represent measurements from fabricated SR solar cells of 180 µm, 130 µm and 100 µm thickness. The simulation is based on electrical characteristics measured on SR solar cells with a standard thickness of 180 µm and efficiencies well above η = 14 % [2]. By decreasing the thickness from d = 180 µm to 100 µm the simulation calculates a decline ΔJ_{SC} = -0.65 mAcm^{-2} and ΔV_{OC} = -6 mV. Our experimental results are in good agreement with the simulation. For thicknesses above d = 100 µm the reduction in current and voltage is almost linear. We expect a relative efficiency loss of $\Delta\eta$ = -0.3 % for cells with d = 100 µm thickness compared to cells with d = 180 µm. However, fabricated cells show an efficiency loss $\Delta\eta$ = -0.6 %. This excess loss is due to a fill factor reduction, which arises from locally high contact resistance between silver and silicon at the front side of the solar cells. The fill factor loss stems from lateral temperature inhomogeneities over the solar cell area during the firing of the front contact grid.

Measurements on solar cell cross sections made by a 3D microscope reveal a thickness variation of up to ± 40 µm throughout the wafer. The thickness variation results in locally varying peak temperatures on a single wafer during firing and thus in an inhomogeneous contact formation. Measurements of the local contact resistance confirm a correlation to the wafer thickness. Therefore, we expect that improved wafer thickness homogeneity will result in more stable solar cell processing, thus allowing for an overall efficiency increase.

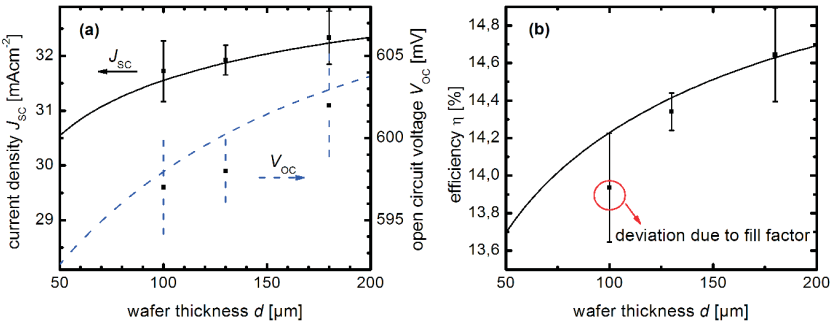

Figure 1:
String Ribbon solar cell measurement results and PC1D simulation for varying mean wafer thickness. a) Thickness reduction from d = 180 µm to 100 µm results in a decline in current density ΔJ_{SC} = -0.65 mAcm^{-2}, voltage ΔV_{OC} = -6 mV. b) Efficiency decreases by $\Delta\eta$ = -0.3 %.

References:

[1] R. M. Swanson, *Prog. Photovoltaics Res. Appl.*,**14**, 443 (2006)
[2] M. Reuter, *"Thin Crystalline Silicon Solar Cells"*, PhD thesis, Stuttgart, p. 56, in press

9.5 % Gain by Dynamic String Interconnection of PV Modules

Author: T. Wurster
In collaboration with: M. B. Schubert and R. Merz

Inhomogeneous illumination, e.g. due to partial shading of one photovoltaic (PV) module in a PV string, limits the common current of all modules of the string. Partial shading may significantly reduce the output voltage of the string by activating a bypass diode of the affected module causing a lower maximum power point (MPP) voltage. The parallel connection of strings forces the inverter to operate all strings at the new reduced MPP voltage of this string, or at the higher MPP voltage of the remaining strings. Both operating points lead to high mismatch losses [1] of the whole system which add upon the mere shading loss of the affected string. To avoid such mismatch losses, the novel Dynamic String Interconnection [2] enables independent MPP tracking of multiple PV strings.

Figure 1a presents the Dynamic String Interconnection (DSI) in buck converter configuration. The DSI sequentially connects each of the strings S_X (X = 1 to 4) to the converter. To operate each string at its individual MPP, the control unit varies the time period $T_{ON,X}$ that connects each string to the converter. The variation of $T_{ON,X}$ adjusts the charge of the capacitance C_X and thereby the string voltage V_{SX} in order to operate S_X at its optimum individual MPP voltage. Figure 1b compares the operation of a PV test system in DSI mode and in parallel connection. For $t < t_1 = 7.5$ min, the graph shows the measured overall efficiencies of the test system without partial shading. The inverter optimizes the operation of the PV system in parallel mode to an efficiency $\eta_{PC}\,(t < t_1) = 4.20$ %. In DSI mode, the system reaches an efficiency $\eta_{DSI}\,(t < t_1) = 4.25$ %, corresponding to a gain $G = 1.2$ %. For $t > t_1$, Fig. 1a displays the efficiencies under partial shading conditions. In the parallel mode, the inverter tracks the PV system to an efficiency $\eta_{PC}\,(t > t_1) = 3.67$ %, while the DSI mode boosts the efficiency to $\eta_{DSI}\,(t > t_1) = 4.05$ %.

The efficiency of the system in DSI mode decreases by only 5 % under partial shading, which is exactly the power share that the shaded module could contribute to the total power of the 20 modules of the system. Under partial shading, the efficiency gain by DSI relative to the parallel mode is $G\,(t > t_1) = 9.5\,\%$.

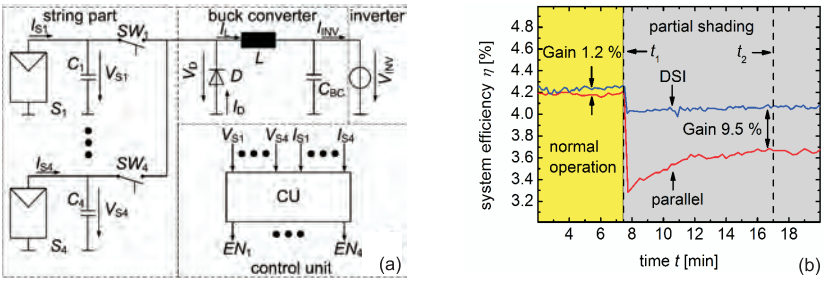

Figure 1:
Schematic and results. a) The string part consists of X PV strings S_X, X capacitors C_X connected in parallel to the strings, and X switches SW_X in series to each of the strings to connect them to the buck converter. The inductance L of the converter transfers and stores the energy E_X of string S_X during a period $T_{ON,X}$. After $T_{ON,X}$ the diode D maintains the transfer of E_X to the inverter. The control unit CU measures the voltages V_{SX} and currents I_{SX} to calculate the momentary power of each string and track it to its individual MPP. b) Performance of 4 PV strings operating in parallel or DSI mode. The efficiency η_{DSI} $(t < t_1) = 4.25\,\%$ in DSI mode is about 1.2 % higher than the efficiency η_{PC} $(t < t_1) = 4.2\,\%$ in parallel mode. The shading of one module in DSI mode lowers the efficiency at t_1 = 7.5 min to η_{DSI} $(t > t_1) = 4.05\,\%$ which is 9.5 % higher than in parallel connection. Moreover, the tracking in DSI is much faster than in the parallel mode.

References:

[1] B. Koirala, B. Sahan and N. Henze, in *Proc. 24th EU PVSEC* (WIP, Munich, 2009), p. 3727

[2] R. Merz, A. S. Garamoun, T. Wurster, J. Jochen, M. B. Schubert, in *Proc. 24th EU PVSEC* (WIP, Munich, 2009), p. 3673

Phosphorus Out-diffusion in Liquid Silicon

Author: S. J. Eisele
In collaboration with: J. R. Köhler, G. Bilger, and M. Dahlinger

The *ipe* developed a laser doping process for η = 18.9% efficient crystalline silicon solar cells [1], as well as for industrial solar cells with selective emitters [2]. We also presented a numerical model, which describes laser induced dopant atom in-diffusion from a precursor into liquid silicon as well as the evaporation and condensation of the precursor layer [3]. The present work extends this numerical model by applying the possibility of out-diffusion of already incorporated dopant atoms. A comparison of experimental and simulation results allows us to determine the out-diffusion coefficient of phosphorus atoms in liquid silicon for the first time.

Our experiments use 0.2 Ωcm p-type silicon wafers with furnace diffused 60 Ω/sq n-type phosphorus doped emitter. After P-glass layer removal, laser irradiation with a pulsed frequency doubled Nd:YAG-laser melts the silicon surface. By varying the number N_S of laser scans at constant pulse energy density E_P = 0.91 $J\text{cm}^{-2}$, we examine the activation of phosphorus atoms as well as their out-diffusion. Figure 1 shows the influence of the number of laser scans N_S on the emitter sheet resistance ρ_S at a constant pulse energy density E_P = 0.91 $J\text{cm}^{-2}$. During the first 10 laser scans N_S the sheet resistance ρ_S drops to ρ_S = 15 Ω/sq, a further increase in N_S results in an increase of ρ_S to ρ_S = 47 Ω/sq, proving the existence of laser induced out-diffusion. Figure 2 depicts the doping profiles, measured by Secondary Ion Mass Spectrometry (SIMS) and, in addition, the simulation results, which are in good agreement with the experimental results. The phosphorus out-diffusion coefficient determined is D_{out} = 8 cm/s, with an accuracy ΔD_{out} = ± 1 cm/s. Further experiments with different laser pulse energy density indicate that the out-diffusion coefficient is independent of the temperature of liquid silicon.

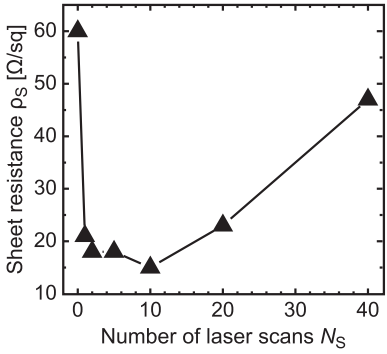

Figure 1:
Repeated pulsed laser melting of furnace diffused phosphorus emitter with sheet resistance ρ_S = 60 Ω/sq at a constant pulse energy density E_P = 0.91 J cm^{-2}. Increased of number of laser scans first reduce the emitter sheet resistance down to ρ_S = 15 Ω/sq, but a further increase of N_S results in an increase of ρ_S up to ρ_S = 47 Ω/sq.

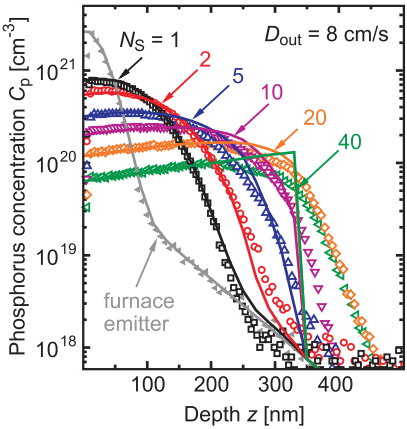

Figure 2:
Doping profiles of laser irradiated furnace emitters from Fig. 1, measured by SIMS, together with the corresponding simulation results. The increase of the number of laser scans results in a change of the shape of the doping profile. The simulation results enable the determination of the phosphorus out-diffusion coefficient D_{out} = 8 cm/s in liquid silicon.

References:

[1] S. J. Eisele, T. C. Röder, J. R. Köhler, and J. H. Werner, Appl. Phys. Lett. **95**, 133501 (2009)

[2] T. C. Röder, S. J. Eisele, P. Grabitz, C. Wagner, G. Kulushich, J. R. Köhler, and J. H. Werner, Prog. Photovolt.: Res. Appl. **18**, 505 (2010)

[3] J. R. Köhler and S. J. Eisele, Prog. Photovolt.: Res. Appl. **18**, 334 (2010)

30 µm wide Laser Transferred Contacts on Silicon Solar Cells

Author: E. Hoffmann
In collaboration with: T. C. Röder, J. R. Köhler, and J. H. Werner

Laser transferred contacts (LTC) enable low finger widths $w < 30$ µm without high temperature steps and heavy metals such as cadmium or lead. The transferred metal contacts the emitter through the anti reflective coating (ARC). Nickel/copper electroplating thickens the contacts, increasing the conductivity of the fingers. First solar cells with an efficiency $\eta = 17.4\%$ and fill factor $FF = 77.7\%$ demonstrate the potential of LTC.

Figure 1 shows the formation of LTC. In step 1, a one sided nickel coated transparent substrate is placed on top of the wafer. Using the laser induced forward transfer (LIFT) process [1] nickel is transferred by local irradiation with a pulsed laser from a glass substrate. The local heating melts the nickel, starting at the substrate/nickel interface.

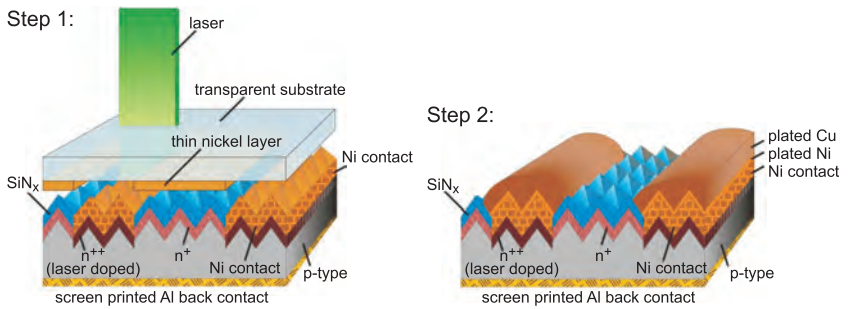

Figure 1:
Laser transferred contacts (LTC) process. In step 1, a glass substrate coated with nickel is placed on top of the cell. A pulsed laser transfers the nickel through the ARC forming the contact. In step 2, electroplating thickens the contact fingers, thus increasing the conductivity.

When the substrate at the interface starts to evaporate, the resulting gas pressure blasts the liquid nickel from the glass support through the ARC. The transferred nickel forms a contact to the emitter with contact resistivity $\rho_C < 1$ mΩcm^2. The width of the laser pulse specifies the contact width w, allowing $w < 10$ µm. In step 2, nickel/copper plating increases the line width. Nickel acts as diffusion barrier for copper, while copper increases the specific conductivity to $\rho = 1.8 \times 10^{-6}$ cm. Electroplating also increases the line width and height with aspect-ratios $a > 0.25$ and line widths $w < 30$ µm.For solar cell production, we use 200 µm thick p-type Czochralski grown Si wafers with KOH etched random pyramid textured surface. Selective laser doping [2] increases the emitter depth locally under the contact finger area. During LTC formation nickel penetrates to a depth $d > 400$ nm into the wafer surface, thus shunting shallow standard furnace diffused emitters. Laser doping deepens the emitter to $d \approx 1$ µm, preventing the metal to contact the p-type bulk material. SiN_x ARC is deposited by plasma enhanced chemical vapor deposition; Aluminum screen printing and firing forms the back contact.

First solar cells show a short circuit current density $J_{SC} = 36.5$ mA/cm^2 and a fill factor $FF = 77.7\%$ on a cell area $A = 4$ cm^2. The contact area amounts up to $A_{cont} = 0.24$ cm^2. The open circuit voltage $V_{OC} = 612$ mV limits the cell efficiency as a result of a not yet optimized selective laser doped area underneath the contacts. In these first experiments, the width w of the laser doped area was $w = 150$ µm and, therefore significantly wider than the width of the LTC. Laser doping increases the reflectivity and Auger-recombination and, therefore should be minimized. Matching the laser doped area to the contact area as well as optimizing the grid design promise further improvements by increasing both J_{SC} and V_{OC}.

References:

[1] J. Bohandy, B.F. Kim, and F. J. Adrian, J. Appl. Phys. **60**, 1538, (1986)
[2] T. C. Röder, S. J. Eisele, P. Grabitz, C. Wagner, G. Kulushich, J. R. Köhler, and J. H. Werner, Prog. Photovolt: Res. Appl. **18**, 505 (2010)

Modelling of the Laser Transfer Process

Author: T. C. Röder

Standard screen printing front side metallization for silicon solar cells limits the width w of the front contact fingers to $w > 100$ µm. The large finger width masks the underlying cell area, thus decreasing the short circuit current I_{sc}. Our laser transferred contacts (LTC) achieve finger widths $w < 30$ µm [1], resulting in less metallized area. A pulsed laser heats, melts and finally transfers a thin nickel layer from a transparent substrate directly through the anti-reflection coating of a solar cell [2].

We numerically solve the heat transport equation in two dimensions to model the temperature profiles in the metal layer and transparent glass substrate. For thin nickel layers, the gas pressure that is necessary to transfer the liquid nickel from the glass to the solar cell surface, arises from *evaporated glass* at the nickel/glass interface. Figure 1 presents three microscope pictures of a 34 nm thick nickel layer after laser irradiation with different pulse energy densities E_p. Figure 1a) shows a nickel layer irradiated with $E_p = 0.15$ J/cm^2; no deformation of the layer is visible.

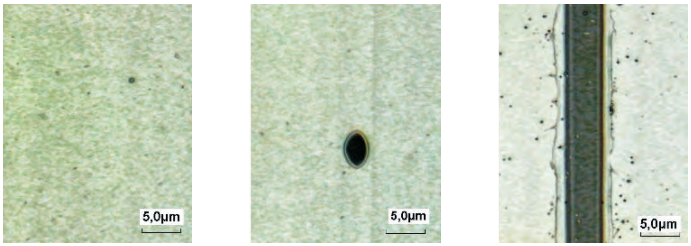

Figure 1:
Microscope pictures of a 34 nm thick nickel layer after laser irradiation with different pulse energy densities E_p. a) no deformation of the nickel layer visible. b) nickel layer deformation indicates melting. c) nickel transfer starts at $E_p = 0.53$ J/cm^2.

Increased E_p = 0.30 J/cm^2 in Fig. 1b) results in the deformation and random local layer ablation. Figure 1c) illustrates the onset of metal transfer at E_p = 0.53 J/cm^2. Figure 2 shows the modelled temperature profiles for the three different pulse energy densities. For E_p = 0.15 J/cm^2, the laser energy is too low to melt the nickel layer, thus no deformation is visible in Fig. 1a). The deformation in Figure 1b) results from complete layer melting. The temperature T of the nickel layer irradiated with E_p = 0.53 J/cm^2 reaches $T \approx 2400$ K well below the boiling point of nickel T_{boil} = 3186 K. Therefore the required transfer gas pressure has to result from evaporated glass.

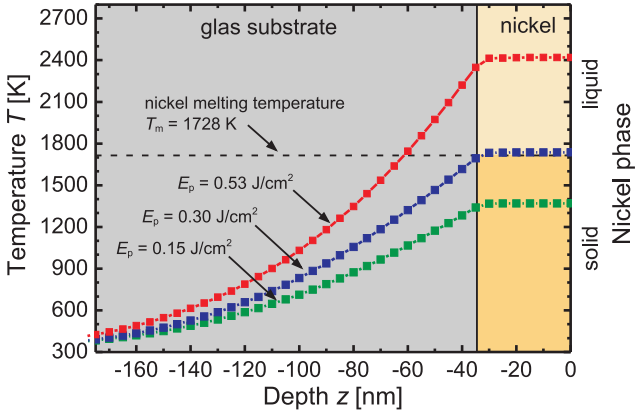

Figure 2:
Modelled temperature profiles for a 34 nm thick nickel layer. At pulse energy density E_p = 0.15 J/cm^2 the nickel temperature is below the melting point. At E_p = 0.30 J/cm^2 the layer melts. Nickel transfer starts at E_p = 0.53 J/cm^2 with temperature T ≈ 2400 K.

References:

[1] T. Röder, E. Hoffmann, J. R. Köhler, and J. H. Werner, in *Proc. 35th IEEE Photov. Spec. Conf.* (IEEE, Piscataway, NY, 2010), in press

[2] J. Bohandy, B. F. Kim, and F. J. Adrian, *J. Appl. Phys.* **60**, 1538 (1986)

Structured Ribbons for Short Circuit Current Gain in Modules

Author: G. Gläser
In collaboration with: L. Hamann and L. Prönneke

The short circuit current gain of silicon solar modules is reduced by several optical losses: i) shading by busbars and grid fingers, ii) reflection of light in the module glass and in the EVA sealing foil, iii) absorption of light in the window layers. Structured ribbons are one approach to minimize the loss of shadowing and reflection for contacting solar cells in a module instead of conventional flat ribbons [1]. Structured ribbons make use of the effect of total internal reflection (TIR). Figure 1 shows the schematic cross section of a conventional flat ribbon (right side) and a structured ribbon (left side). In a conventional flat ribbon, the impinging radiation is reflected back and lost. The triangular texture of the structured ribbon reflects light impinging perpendicularly at an angle such that total internal reflection at the module glass occurs. As a consequence, the radiation is guided to the adjacent active cell areas and converted into electrical energy. The critical angle of total internal reflection is $\beta_{TIR} = 41.8°$. We manufacture single cell modules using 6” monocrystalline silicon solar cells with structured ribbons.

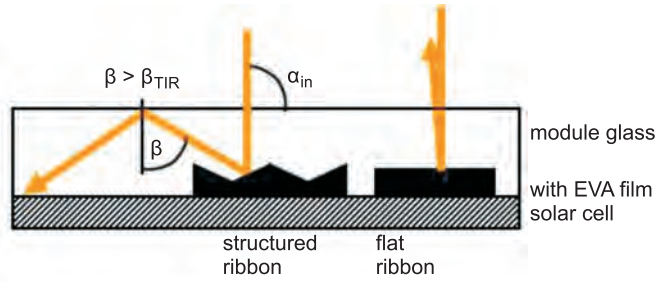

Figure 1:
The triangular shape of the ribbon (left side) reflects perpendicular light at an angle $\beta > 41.8°$ with the consequence of total internal reflection at the inner surface of the module glass. It is reflected back on the cell's active surface. Perpendicular light impinging on a conventional flat ribbon (right side) is lost.

As a reference, we assemble modules with conventional flat ribbons. Electroluminescence images of all modules ensure, that the measurements are only carried out on homogeneous and therefore comparable module areas. Figure 2 presents the external quantum efficiencies (*QE*) on a structured ribbon (red line) and a flat ribbon (green line) of the encapsulated solar cell.The overall short circuit current of the modules is J_{SC} = 34.6 mA/cm^2. A conventional flat ribbon shows about 7 % quantum efficiency leading to a short circuit current density of J_{SC} = 1.8 mA/cm^2. The structured ribbon reaches significantly higher quantum efficiencies than the flat ribbon. Between λ = 400 and 1000 nm the *QE*-values reach up to 33 %, thus yielding J_{SC} = 12.8 mA/cm^2 and a difference of 11 mA/cm^2 compared to the flat ribbon. As the ribbons shadow 4 % of cell area, they lead to an overall increase of the module's short circuit current of Δ J_{SC} = 0.44 mA/cm^2. That results in a relative enhancement of 1.27 % in current density for the module with J_{SC} = 34.6 mA/cm^2 on its active cell area and in a raise in efficiency of 0.2 % absolute for an η = 16 % cell.

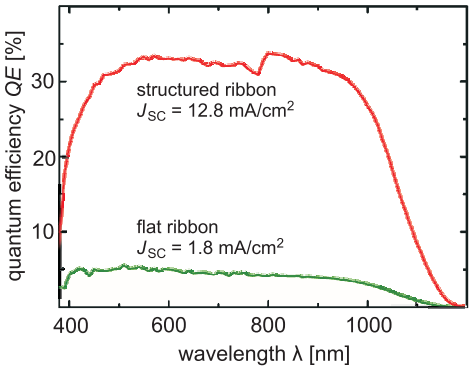

Figure 2:
External quantum efficiency measurements on a structured ribbon (red line) and a conventional flat ribbon (green line) of the encapsulated solar cell.

References:

[1] E. M. Sachs, J. Serdy, A. M. Gabor, F. van Mierlo, T. Booz, in *24th EU PVSEC*, (WIP, Munich, 2009), p. 3222

Optimized Front Side Grids for Solar Cells

Author: G. Kulushich
In collaboration with: R. Zapf-Gottwick

Balancing the efficiency losses on the front side of a solar cell due to the optical shadowing of the front grid, the electrical resistances and the emitter recombination, we show a direction of how the front side of a solar cell has to change to gain in efficiency.

Figure 1 illustrate the relative losses in efficiency $\Delta\eta_{loss}/\eta^*$ associated with the front side of solar cells compared to an “ideal” efficiency η^* without front side losses. We consider the efficiency losses for cells with conventional doped emitter with a sheet resistance R_{sh} = 60 Ω/sq in Fig.1a; and for cells with selective emitter with R_{sh} = 100 Ω/sq in Fig.1b. The seven paired bars represent the optical loss due to the finger and busbar shadowing; the electrical loss due to sheet R_{sh}, contact R_c, finger line R_f, and busbar line R_b resistances; and the electronic loss due to recombination in the emitter bulk, emitter surface, and emitter/metal interface. The Auger limit in the hole diffusion length L_h gives the bulk recombination. The front surface recombination velocity S_f expresses the surface/interface recombination rate. The paired bars in each group represent the losses of the not-optimized and optimized grid. Optimization is done by minimizing the losses due to the front grid. The not-optimized cells have a standard industrial screen printed front grid design. One assumption is a constant aspect ratio of the fingers to account for the screen printing technique. The calculation shows that the efficiency increases by replacing the two standard screen printed busbars by at least five busbar wires which connect only the fingers but have no intimate contact to the emitter.

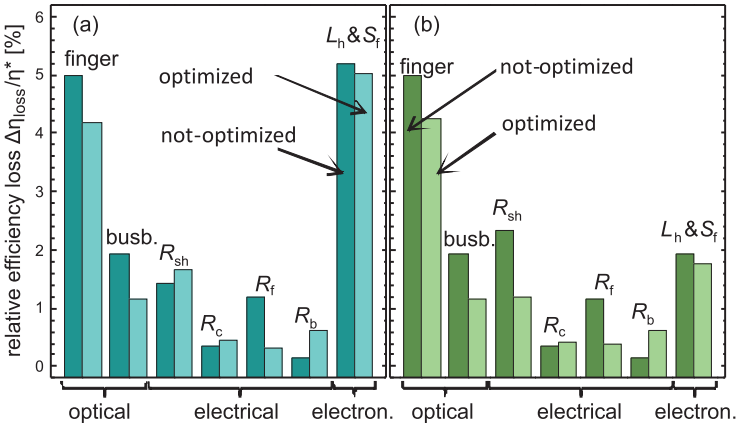

Figure 1:
Calculated relative efficiency losses $\Delta\eta_{loss}/\eta^*$ due to frontside: optical by finger and busbar, electrical by sheet R_{sh}, contact R_c, finger R_f, and busbar line resistance R_b and electronic defined by hole diffusion length L_h and surface recombination velocity S_f for not-optimized and optimized grid for (a) conventional R_{sh} = 60Ω/sq and (b) selective emitter R_{sh} = 100Ω/sq.

On the one hand, more busbars decrease the finger length and their resistances. On the other hand, the busbar line resistance steps up because the busbar wires have a smaller cross section compared to the screen printed busbars. The electronic losses take the other large part of the efficiency losses. With a higher sheet resistance, the emitter Auger recombination decreases and the electronic loss of the selective emitter cells gets significantly smaller compared to the conventional cells. The decrease in electronic loss by optimizing the grid design is because of the reduced interface recombination loss due to a smaller grid/emitter contact area. Losses due to the sheet resistance of selective emitter cells reduce with a smaller finger distances. Optimization of the front grid changes the conventional busbar design to a grid with multiple busbars realized by wires. This design predicts an efficiency gain $\Delta\eta$ = 0.4 % for conventional and $\Delta\eta$ = 0.6 % for selective emitter cells.

Photoluminescence from Silicon Nanocrystals?

Author: J. Kistner
In collaboration with: C. Chen and M. B. Schubert

In 1990 Canham observed visible photoluminescence (PL) of silicon nanocrystals (nc-Si) in porous silicon [1]. For grain sizes below 6 nm, luminescence with energies far above the band gap of c-Si occurred, which Canham ascribed to quantum mechanical effects. Decreasing grain sizes led to a spectral blue shift of the PL. Since 1990 various researchers reported on the fabrication of nc-Si. Photoluminescence throughout the complete visible spectrum always was ascribed to nc-Si. However, the origin of the nc-Si luminescence has not been completely understood.

In order to observe and understand the PL of nc-Si, a few of these fabrication approaches are successfully re-investigated by us. These former approaches assumed that excess Si in amorphous silicon alloys such as silicon rich nitride (SRN) and oxide (SRO) was available for nc-Si formation [2, 3]. Consequently, the complete visible spectrum should be observable upon varying the Si content in these alloys. Even though our experiments reconfirm the experimental findings of other authors, we prove that the observed PL *does not* originate from nc-Si.

Figures 1(a) and (b) show the PL spectra under 325 nm excitation of the SRN and SRO layers with different Si content. The observed PL ranges from the near infrared to the blue spectral region covering the complete visible spectrum. As expected, a spectral blue-shift occurs for decreasing Si content. However, high resolution transmission electron microscope analysis proves that the luminous samples do not contain any nc-Si but are completely amorphous.

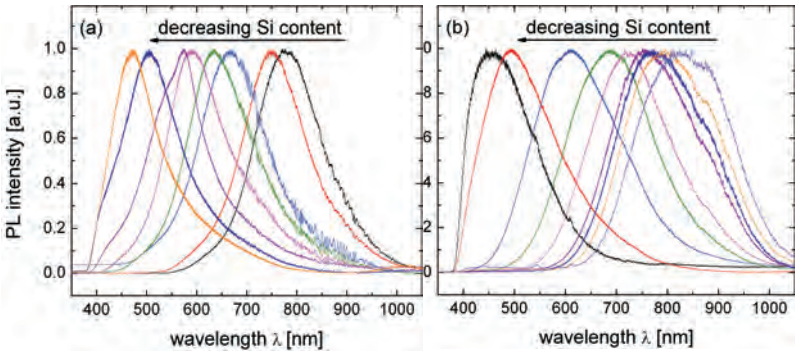

Figure 1:
PL spectra of (a) SRN and (b) SRO layers with different Si-contents. The complete visible spectrum is covered by the PL of these silicon alloys. A decrease of the Si content results in a spectral blue-shift. In contrast to various reports, the observed PL, cannot be ascribed to nc-Si but to the amorphous structure of the alloys.

We ascribe the observed PL to recombination between band-tail states. Dunstan gave an arithmetic expression for the so called band-tail luminescence of amorphous Si [4]. Application of this luminescence model predicts the observed PL of our SRN and SRO layers.

Thus, our experiments prove that PL from SRN or SRO alloys originates from band-tails. The pure existence of nc-Si in such layers as reported elsewhere gives no link between the observed PL and quantum mechanical effects. Consequently, SRN and SRO are inappropriate matrices to study PL from nc-Si.

References:

[1] L. T. Canham, Appl. Phys. Lett. **57**, 1046 (1990)
[2] L. V. Mercaldo, P. D. Veneri, E. Esposito, E. Massera, I. Usatii, and C. Pivato, Mat. Sci. and Eng. B **159-160**, 77 (2009)
[3] T. Y. Kim, N. M. Park, K. H. Kim, G. Y. Sung, Y. W. Ok, T. Y. Seong, and C. J. Choi, Appl. Phys. Lett. **85**, 5355 (2004)
[4] D. J. Dunstan, Sol. Stat. Comm. **43**, 341 (1982)

Ideality Factor Extraction from Photoluminescence Images

Author: L. Stoicescu
In collaboration with: G. C. Gläser, M. Reuter, U. Rau, and J. H. Werner

The ideality factor *n* is an indicator for the quality of a solar cell, where higher efficiencies are generally associated with ideality factors *n* close to unity. Ideality factors are generally determined from current/voltage (I/V) measurements [1] as well as measurements of the open circuit voltage (sunsVoc) [2] or the charge carrier density (sunsPL) under varying light intensities. The main disadvantage of these methods is that they determine *n* for the whole cell as a fitting parameter to the one or two diode model. The influence of locally dominant recombination mechanisms is lumped into one 'global' ideality factor, making it difficult to locate them and understand their origin. In contrast photoluminescence (PL) images allow contactless measurements of the ideality factor with high local resolution. The method can be applied to wafers at any processing stage; thus it is of substantial benefit for the understanding, developing and process monitoring of solar cells.

Under open circuit conditions of the cell/wafer, a camera captures two PL images $\Phi_{1,out}$ and $\Phi_{2,out}$, while a laser excites the sample uniformly with a different intensities $\Phi_{1,in}$ and $\Phi_{2,in}$ for each picture. We compare the laser induced recombination current density to the measured PL intensity and calculate the ideality factor image, displaying the local ideality factor

$$n_{PL}(x) = \ln\left(\frac{\Phi_{1,out}(x)}{\Phi_{2,out}(x)}\right) \Big/ \ln\left(\frac{\Phi_{1,in}(x)}{\Phi_{2,in}(x)}\right) \qquad (1)$$

at every point *x* of the sample. In this case $n_{PL}(x)$ describes the injection dependence of the recombination. During the calculation, all calibration constants cancel out and thus no further calibration is needed.

Figure 1 displays the PL image of high efficiency passivated emitter and back with rear local Al contacts (PERC) cells on a c-Si wafer. For some cells, the mask for the front side oxide passivation and emitter is mismatched against the mask for the backside passivating oxide. The unaffected homogeneous cells are surrounded by a dashed square. Figure 2 shows the image of the local ideality factor $n_{PL}(x)$ determined by Eq. (1) for the wafer of Fig. 1. The passivation and doping on the active cell area lead to recombination and injection properties, which result in a lower ideality factor than for the rest of the wafer.

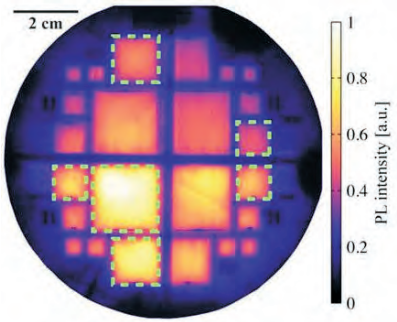

Figure 1:
PL image of PERC cells on c-Si wafer.

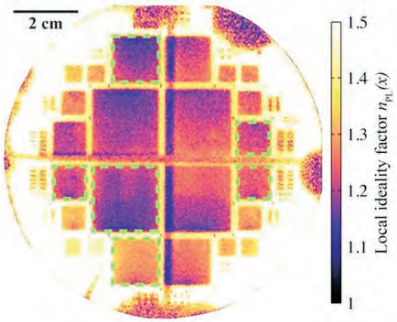

Figure 2:
Ideality image of PERC cells in Fig. 1. We obtain a good correlation with a standard deviation of only 0.04 between the mean local ideality factor and the global ideality factor determined from I/V measurements of homogeneous PERC cells [3].

References:

[1] J. H. Werner, Applied Physics A **47**, 291 (1988)
[2] M. J. Kerr, A. Cuevas, Solar Energy **76**, 263 (2004)
[3] L. Stoicescu, G. C. Gläser, M. Reuter, U. Rau and J. H. Werner, in *Proc. 25th EU PVSEC* (WIP, Munich, Germany, 2010), in press

Improved Laser Edge Isolation Process for Silicon Solar Cells

Author: A. Bertram
In collaboration with: J. R. Köhler and K. Carstens

Laser technologies enable fast and accurate processing of solar cells. One of these processes is laser edge isolation (LEI), the disjunction of the emitter at the cell edge which occurs during diffusion. For a sufficient isolation the parallel resistance R_P characterizes the quality of the LEI process. An R_P > 3 kΩcm^2 is needed for good solar cell performance [1]. Based on the results in Ref. [1], LEI is chosen to be on the front side of the solar cells. Key parameters for LEI are the focus position, the overlap of the single pulses, and the laser pulse energy density. This contribution examines, for the first time, the influence of the focus position on R_P. The focus positions f_p on the wafer front side are at different distances above and underneath the wafer surface. We achieve the best R_P > 10 kΩcm^2 with a f_p = 600 µm above the wafer. Figure 1a depicts a laser groove of width $w \approx 70$ µm and depth $d \approx 35$ µm. The microscope image in Fig. 1b shows that a focus at the surface only generates “weld seams” in silicon, but no ablation at all.

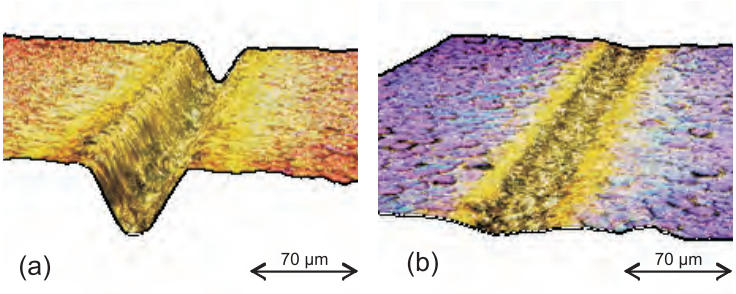

Figure 1:
3D images of laser grooves on a crystalline silicon wafer. a) focus position 600 µm above the surface, depth of the laser groove: 38 µm; width: 72 µm b) focus position on the surface.

Figure 2 shows the dependence of the groove depth *d* on the focus position f_p. We explain the step like increase of *d* above a focus position f_p > 300 µm with the strong absorption of laser radiation in evaporated silicon above the wafer surface, which strongly heats the silicon vapor. The over-heated silicon vapor creates a high vapor pressure and pushes out the underlying silicon melt. Figure 3 illustrates the process, which is most likely the reason for the strong focus position dependence of our optimized laser edge isolation process. Table 1 compares solar cells with LEI and mechanically cut edges. The results prove the effectiveness of the improved laser edge isolation process.

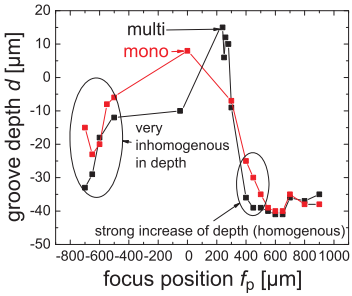

Figure 2:
LEI groove depth increases strongly if focus distance to wafer surface exceeds 300 µm.

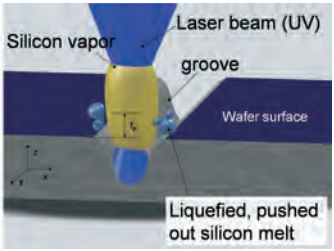

Figure 3:
Physical process of silicon vapor induced ablation.

Table 1: Parameters of laser edge isolated string ribbon solar cells.

	η [%]	FF [%]	R_S [Ωcm^2]	R_P [kΩcm^2]
Laser edge isolated	14.9	75.9	1.01	46
Cut-off edges (2 mm)	14.8	76.0	0.97	55

References:

[1] E. Schneiderlöcher, *Laserstrahlverfahren zur Fertigung kristalliner Silizium - Solarzellen*, PhD, Universität Freiburg, 2004, pp. 130

[2] *D. Kray*, Sol. Energy Mater. Solar Cells **94**, 830 (2010)

Temperature and Irradiance Effects on Outdoor PV Performance

Author: B. Zinßer
In collaboration with: G. Makrides, M. B. Schubert, and G. E. Georghiou**

For predicting the annual energy yield of photovoltaic (PV) systems at real operating conditions, the most important quantities are the nominal power in the field P_{field}, the irradiance and temperature dependencies. Usually, the module data sheet only provides rated power P_N and power temperature coefficient γ at standard test conditions (STC: irradiation $G = 1000\ W/m^2$ and module temperature $T_{module} = 25\ °C$). Figure 1 illustrates how we determine all three parameters for twelve different PV technologies from one year outdoor field data in Stuttgart and in Nicosia.

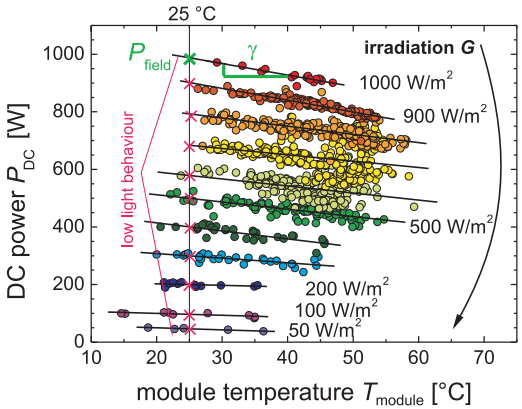

Figure1:
The DC power output of PV systems declines with rising module temperature. All data are filtered to an optical path length equivalent to AM 1.5. Evaluating the outdoor data yields the DC power P_{field} at STC, the DC power temperature coefficient γ, and the low light performance of the different PV technologies.

*University of Cyprus - Photovoltaic Technology

The figures 2a and 2b comprehend results on all PV systems investigated in Stuttgart. The better low light behavior of three thin film technologies yields a 3 % surplus in the annual energy yield, similar in Stuttgart and in Nicosia. The better temperature coefficient of thin films raises the annual yield by 1.4 % in Stuttgart, and by 4 % in the hotter Nicosia.

In conclusion, however, the apparent surplus in annual energy yield of the thin film technologies deduced above is lower than usual measurement uncertainties for energy measurement and nominal power determination.

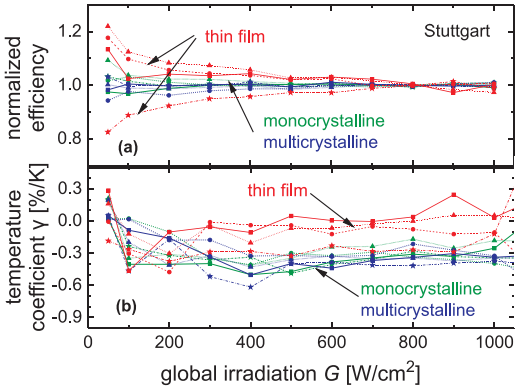

Figure 2:
a) The low light efficiency of crystalline silicon PV modules is almost constant. The amorphous Si and CdTe thin film modules enhance their efficiency at low light levels while the efficiency of CIGS modules decreases. (b) The temperature coefficient of the DC power is independent of the solar irradiation. The thin film modules exhibit a more favorable temperature coefficient than the crystalline Si ones.

References:

[1] Live data web page: www.ipe.uni-stuttgart.de/pvsystem
[2] B. Zinßer, G. Makrides, M. B. Schubert, G. E. Georghiou, and J. H. Werner, in *Proc. 35th Photov. Spec. Conf.* (IEEE, Piscataway, NY, 2010) in press

Publikationen
Publications

Shunt Detection in Amorphous Silicon Modules by *I/V*-Measurements
M. A. Bouattour, A. Al Tarabsheh, I. Radev, M. B. Schubert
in *Proc. 25th Europ. Photovolt. Solar Energy Conf.* (*WIP, Munich, 2010*),
pp. 2924 - 2927, in press, doi: 10.4229/25thEUPVSEC2010-3AV.1.15

Novel Texture for String Ribbon Silicon Solar Cells
J. Cichoszewski, M. Lipinski, F. Schwerdt, and M. Reuter,
in *Proc. 25th Europ. Photovolt. Solar Energy Conf.* (*WIP, Munich, 2010*),
pp. 2357 - 2359, in press, doi: 10.4229/25thEUPVSEC2010-2CV.3.79

a-SiC:H Passivation for Crystalline Silicon Solar Cells
C. Ehling, J. H. Werner, M. B. Schubert
Phys. Stat. Sol. C 7, 1016 - 1020 (2010), doi**:** 10.1002/pssc.200982849

Amorphous and Microcrystalline Silicon Based Hetero Back Contact
C. Ehling, L. Hamann, M. B. Schubert
in *Proc. 25th Europ. Photovolt. Solar Energy Conf.* (*WIP, Munich, 2010*),
pp. 2186 - 2189, in press, doi: 10.4229/25thEUPVSEC2010-2CV.3.34

Nanometer Thin Sputtered Phosphorus Layers for Laser Doped Solar Cells
S. Eisele, M. Sämann, and G. Bilger,
Surf. Interface Anal. 42, 1573 - 1574 (2010) , doi: 10.1002/sia.3580

Influence of Precursor Layer Ablation on Laser Doping of Silicon
J. R. Köhler, and S. Eisele,
Progr. Photovolt. Res. Applic. 18, 334 (2010) , doi: 10.1002/pip.968

Potential of Photovoltaic Systems in Countries with High Solar Irradiation
G. Makrides, B. Zinßer, M. Norton, G. E. Georghiou,
M. B. Schubert, and J. H. Werner,

Renew. Sustain. Energy Rev. 14, 754 - 762 (2010), doi: 10.1016/j.rser.2009.07.021

Degradation of Different Photovoltaic Technologies under Field Conditions
G. Makrides, B. Zinßer, G. E. Georghiou, M. B. Schubert, and J. H. Werner, in *Proc. 35th IEEE Photovoltaic Specialists Conf.* (*IEEE Publishing Service, Piscataway, NY, 2010*) in press

Modelling the Power Output and Energy Yield of 13 Different Photovoltaic Systems
G. Makrides, B. Zinßer, G. E. Georghiou, M. B. Schubert, and J. H. Werner, in *Proc. 25th Europ. Photovolt. Solar Energy Conf.* (*WIP, Munich, 2010*), pp. 4682 - 4687, in press, doi: 10.4229/25thEUPVSEC2010-4BV.1.89

Outdoor Performance Evaluation of Grid-Connected PV technologies in Cyprus
G. Makrides, B. Zinßer, M. Norton, G. E. Georghiou, M. B. Schubert, and J. H. Werner,
J. Energy & Pow. Eng. 4, 52 - 57 (2010)

Evaluation of grid-connected Photovoltaic system performance losses in Cyprus
G. Makrides, B. Zinßer, G. E. Georghiou, M. B. Schubert, and J. H. Werner, Presented at: Med Power, Agia Napa, Cyprus, 52 - 57 (2010)

Optimization of the In Situ Series Connection of Amorphous Silicon Solar Modules on Glass and Foil Substrates
R. Merz, J. Kistner, M. A. Bouattour, and M. B. Schubert
Phys. Status Solidi A 207, 686 - 690 (2010),
doi: 10.1002/pssa.200982850

Heavily Doped Emitter Analysis and Optimization for Crystalline Silicon Solar Cells
V Nguyen, M. Reuter, P. Gedeon, R. Zapf-Gottwick, and J. H. Werner,

in *Proc. 25th Europ. Photovolt. Solar Energy Conf.* (*WIP, Munich, 2010*), pp. 2028 - 2031, in press, doi: 10.4229/25thEUPVSEC2010-2CV.2.86

Thin Solar Cells
M. Reuter
in *Ultra-thin Chip Technology and Applications*, edited by: Burghartz, Joachim (*Springer-Verlag GmbH, Heidelberg, Deutschland, 2010*), in press

Optical Characterisation of Thin Silicon
M. Reuter, and S. Eisele,
in *Ultra-thin Chip Technology and Applications*, edited by: Burghartz, Joachim (*Springer-Verlag GmbH, Heidelberg, Deutschland, 2010*), in press

Add-on laser tailored selective emitter solar cells
T. Röder, S. Eisele, P. Grabitz, C. Wagner, G. Kulushich, J. R. Köhler, and J. H. Werner,
Progr. Photovolt. Res. Applic. 18, 505 - 510 (2010), doi: 10.1002/pip.1007

30 µm Wide Contacts on Silicon Cells by Laser Transfer
T. Röder, E. Hoffmann, J. R. Köhler, and J. H. Werner,
in *Proc. 35th IEEE Photovoltaic Specialists Conf.* (*IEEE Publishing Service, Piscataway, NY, 2010*) in press

Amorphous silicon based p-i-i-n photodetectors for point-of-care testing
M. Sämann, D. Furin, J. Thielmann, A. Pfäfflin, G. Proll, C. Harendt, G. Gauglitz, E. Schleicher, and M. B. Schubert,
phys. stat. solidi (c) 7, 1160 - 1163 (2010), doi: 0.1002/pssc.200982822

Sputtered and Laser Recrystalized Phosphorus-doped Zinc Oxide
M. Sämann, S. Eisele, and G. Bilger,
Surf. Interface Anal. 42, 1570 - 1572 (2010), doi: 10.1002/sia.3610

Ideality Factor Extraction from Photoluminescence Images
L. Stoicescu, G. Gläser, M. Reuter, U. Rau, and J. H. Werner,
in *Proc. 25th Europ. Photovolt. Solar Energy Conf.* (*WIP, Munich, 2010*),
pp. 29 - 32, in press, doi: 10.4229/25thEUPVSEC2010-1AO.4.3

Dynamic String Interconnection with Buck Converter Topology
T. Wurster, R. Merz, and M. B. Schubert
in *Proc. 25th Europ. Photovolt. Solar Energy Conf.* (*WIP, Munich, 2010*),
pp. 4459 - 4462, in press, doi: 10.4229/25thEUPVSEC2010-4BV.1.25

Rating of Annual Energy Yield More Sensitive to Reference Power than Module Technology
B. Zinßer, G. Makrides, M. B. Schubert, G. E. Georghiou,
and J. H. Werner,
in *Proc. 35th IEEE Photovoltaic Specialists Conf.* (*IEEE Publishing Service, Piscataway, NY, 2010*) in press

Lehrveranstaltungen
Lectures

Promotionen
Ph. D. Theses

Diplomarbeiten
Diploma Theses

Studienarbeiten
Major Term Projects

Gäste & ausländische Stipendiaten
Guests

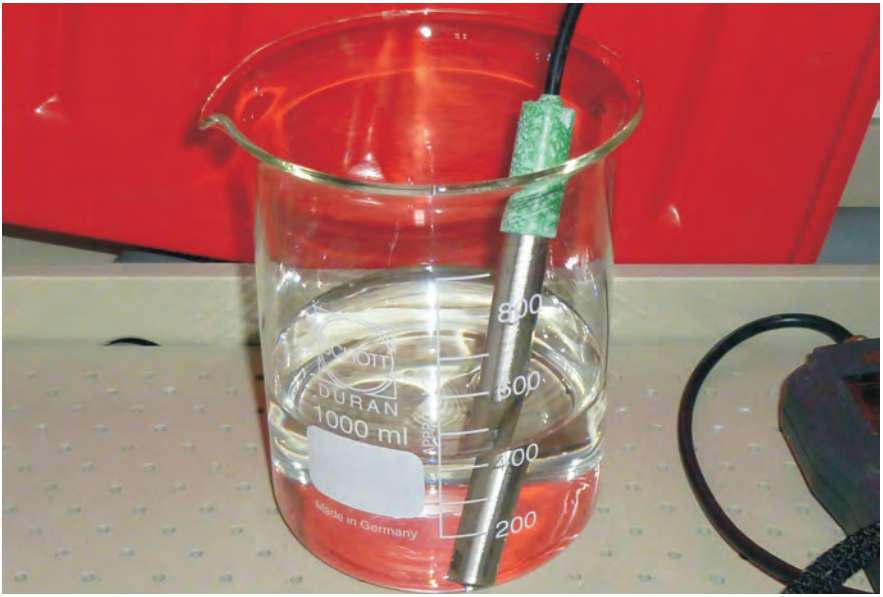

Bauelemente der Mikroelektronik (1. Semester)
J. H. Werner

Energiebänder und Leitfähigkeit
Silicium - der Werkstoff der Mikroelektronik
Elektronen und Löcher in Halbleitern
Ströme in Halbleitern
Nichtgleichgewicht und Injektion
Elektrostatik des pn-Übergangs
Ströme im pn-Übergang

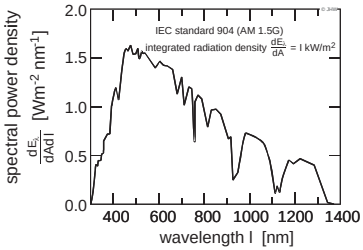

Energiewandlung (6. / 8. Semester)
J. H. Werner

Grundlagen der Kernenergie
Thermodynamik
Direkte Nutzung der Sonnenenergie (Solarthermie, Photovoltaik)
Indirekte Nutzung der Sonnenenergie (Wasserkraft, Windenergie)
Chemische Wandlung und Speicherung elektrischer Energie

Laser and Light Sources (5. / 7. Semester)
J. H. Werner and J. Köhler

The Human Eye
Light and Color
Photometry
Incoherent Light Sources
Light Emitting Diodes
Lasers
Laser Processing

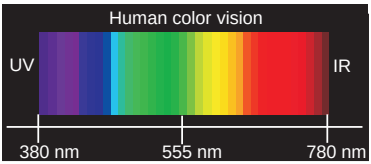

Optoelectronic Devices and Circuits I (4. Semester)
J. H. Werner

Basic physics
Thermal radiation
Coherence
Semiconductor basics
Excitation and recombination processes in semiconductors
Light emitting diodes
Semiconductor lasers
Glass fibers
Photodetectors

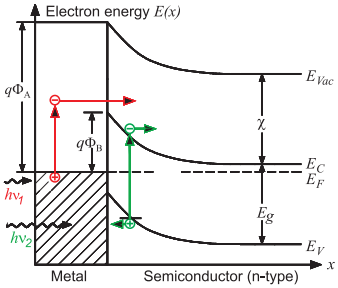

Photovoltaik I (4. Semester)
J. H. Werner

Was die Photovoltaik leisten kann
Der Photovoltaische Effekt: Solarzelle, Solarmodul, Solaranlage
Sonnenspektrum und Energieverbrauch in Deutschland
Maximaler Wirkungsgrad einer Solarzelle
Grundprinzip einer Solarzelle
Ersatzschaltbild der Solarzelle
Photovoltaik-Materialien und –Technologien
Modultechnik
Photovoltaische Systemtechnik
Erträge von Photovoltaiksystemen
Photovoltaik-Markt

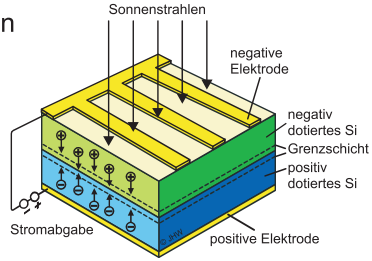

Solid State Electronics (7. Semester)
J. H. Werner

Free electrons as particles and waves
Electronic bands in solids
Band diagrams of semiconductors
Currents in semiconductors
Emission of electrons from metals and semiconductors
The Schottky-contact
Photoeffects in semiconductors

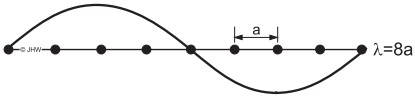

Wissenschaftliches Vortragen und Schreiben I (Wintersemester)
J. H. Werner

Kernbotschaften
Aufbau eines Vortrags
Standardfehler (Strukturfehler, Technikfehler, Fehler im Auftreten)
Praktische Schritte zum Vortrag
Selbst- und Fremdbeurteilung (mit Videoaufzeichung)

Wissenschaftliches Vortragen und Schreiben II (Sommersemester)
J. H. Werner

Kernbotschaften
Aufbau und Elemente einer Publikation
Bilder, Tabellen und Referenzen

Praktische Übungen im Labor „Halbleitermesstechnik“ (7. Semester)
M. B. Schubert

Herstellverfahren von Halbleitern und dünnen Schichten
elektrische Messtechniken zur für Minoritäten und Majoritäten
optische Messtechnik
strukturelle Messtechniken

Promotionen
Ph. D. Theses

Mawuli Ametowobla
Characterization of a Laser Doping Process for Crystalline Silicon Solar Cells

Bastian Zinßer
Jahresenergieerträge unterschiedlicher Photovoltaik Technologien bei verschiedenen klimatischen Bedingungen

Diplomarbeiten
Diploma Theses / Master Theses

Fatih Beyaz
Erarbeitung einer Messmethode der externen Quanteneffizienz von organischen Tandemzellen

Dimitar Ganchev
Kleinleistungs-Solarladeregler mit Maximum Power Point Tracking

Stefan Hieber
Annealing Behavior of Thermally Stable a-SiC:H

Liviu Stoicescu
Aufbau eines Messplatzes zur ortsaufgelösten Charakterisierung von Solarzellen mittels Photolumineszenz

Thomas Wurster
Fortentwicklung der dynamischen Multistrang-Verknüpfung von Photovoltaikmodulen

Studienarbeiten
Major Term Projects

Xiran Chen
Photolumineszenz von Silizium Nanokristalliten in Silizium Nitrid Schichten

Adam Dancs
Siebdrucksolarzellen mit getrenntem Finger- und Busbardruck

Ralf Daubenschmid
Lasertexturierung von Zinkoxid

Lars Hamann
Heterokontakt basierte Solarzellen

Kun Mo
Modellierung hochdotierter Emitterprofile

Ivan Radev
Parallel Resistance of Single Solar Cells in a Laminated a-Si Module

Dorian Treptow
Temperaturstabile a-SiC:H Passivierschichten für Siliziumsolarzellen

Chengzhi Xu
Feinlinien-Metallisierung mit Siebdruck

Gäste & ausländische Stipendiaten
Guests

Anas Al Tarabsheh
The Hashemite University, Zarqa, Jordanien

Li Da
Tongji University , Shanghai, China

Yutaka Hoshina
Tokyo Institute of Technology, Tokyo, Japan

Elaine del Carmen Izquierdo Rivera
Universidad Tecnologica de Panama, Panama

Shinsuke Miyajima
Tokyo Institute of Technology, Tokyo, Japan

Marija Rankovic
University of Belgrade, Serbien

Suttirat Rattanapan
Tokyo Institute of Technology, Tokyo, Japan

Reinhard Schwarz
Instituto Superior Técnico, Lisbon, Portugal

Shinya Yoshidomi
Tokyo University of Agriculture and Technology,
Tokyo, Japan

Was sonst noch war ...
More than Science ...

Mitarbeiterliste
Staff Members

Lageplan
Location Map

Was sonst noch war ...
More than Science ...

Otto F. Scharr-Preis für Energietechnik

Den ersten Preis für *„Praxisbezogene Forschung für zukunftsorientierte Energie-Lösungen“* erhielt in diesem Jahr Erik Hoffmann für seine Diplomarbeit „Laserinduzierte Vorderseitenmetallisierung auf c-Silizium Solarzellen“, welche er in der Forschungsgruppe „Laserprozesse“ am *ipe* angefertigt hat.

Tag der Wissenschaft

Hier konnten Studenten im Rahmen der Vorlesung „Energiewandlung“ wieder zeigen, wie man in Teamarbeit selbst aus scheinbar wertlosen Abfallmaterialien funktionierende Energiewandler konstruiert und baut.

Girls' Day

Erstmals durften zwei „*ipe*-Jungs“, Ali Bouattour und Jakub Cichoszewski, interessierte Nachwuchswissenschaftlerinnen von den Vorteilen der photovoltaischen Energiegewinnung und denen eines ingenieurwissenschaftlichen Studiums überzeugen. Ihre „Meisterprüfung“ im Löten haben auch in diesem Jahr alle mit Bravour bestanden.

Otto F. Scharr-Award for Power Engineering

Erik Hoffmann got the first price for his diploma thesis “Laser-induced front side metallization for crystalline silicon solar cells”.

Tag der Wissenschaft

Part of the lecture “energy conversion” is the construction and built up of energy converters out of waste and broken devices, which were presented during the “Tag der Wissenschaft”.

Girls' Day

The “*ipe* Boy-Group”, Ali Bouattour and Jakub Cichoszewski, did anything to convince a group of high school girls of the benefits to study engineering science. Photovoltaic energy conversion was also a topic of interest. Finally all the girls got their “soldering-master certificate”.

Ferienakademie

Auch dieses Jahr hat die Ferienakademie (www.ferienakademie.de) der Universitäten Stuttgart, Erlangen-Nürnberg und der TU München über 180 erstklassige Studierende in 12 Kursen in die Berglandschaft des Sarntals, Südtirol, gebracht. Die Studenten, die sich nicht nur durch exzellente Noten, sondern (zum Leidwesen mancher Professoren) auch durch eine gute körperliche Kondition auszeichnen, tragen das gesamte wissenschaftliche Programm, das immer wieder von anstrengenden Tageswanderungen unterbrochen ist. Die Akademie finanziert sich zum größten Teil durch Spenden der Industrie.

Jahresabschlussfeier

Mitgefeiert haben auch in diesem Jahr nicht nur *ipe*-Mitarbeiterinnen und Mitarbeiter sondern auch viele ehemalige *ipe*-ler. Hervorragende Verpflegung und ein schonungslos lustiger Jahresrückblick sind immer Gründe, sich dieses Highlight nicht entgehen zu lassen. Wie im letzten Jahr gab es Ende 2009 wieder zahlreiche Auszeichnungen für hervorragende Studien-, Bachelor-, Diplom- und Master-Arbeiten, die am *ipe* durchgeführt wurden.

Summer School

Over 180 of the very best students attended the summer school of the Universities Stuttgart, Erlangen-Nürnberg and the Technical University of Munich in the mountainous landscape of the Sarn-valley in the northern territory of Italy, Alto Adige. Exhausting day hikes were also part of the “scientific” program, a challenge for many professors but a walk over for most of the students. The summer school is funded by donations of different German industrial companies. Please find more details under www.ferienakademie.de.

Company Party

The famous *ipe*-party at the end of each year attracts also former *ipe* colleagues. A good buffet as well as a ruthless retrospective are always good reasons not to miss out this event. Again, many students were awarded for their excellent research thesis.

Mitarbeiterliste

Staff Members

Titel / Name	Telefon 0711 - 685 - ...	E-Mail (vorname.name) @ipe.uni-suttgart.de	Arbeitsgebiet
Leo Bauer	60105	leo.bauer	Metallisierung, Photo-arbeiten, Maskentechnik
Dipl.-Ing. Alexander Bertram	67163	alexander.bertram	Laserbearbeitung, Laser-dotieren, Kantenisolation
Dr.-Ing. Gerhard Bilger	67176	gerhard.bilger	Oberflächenanalytik; Technologie Support
Dipl.-Ing. Mohamed Ali Bouattour	67181	ali.bouattour	Integrierte Photovoltaik
Dipl.-Ing. Jakub Cichoszewski	69219	jakub.cichoszewski	Texturen für Solarzellen
Dipl.-Ing. Christian Ehling	67161	christian.ehling	Amorphe Passivierschichten
Dipl.-Ing. Sebastian Eisele	67198	sebastian.eisele	Laserdotieren
Dipl.-Ing. Panagiotis Gedeon	67182	panagiotis.gedeon	String Ribbon Solarzellen
Dr.-Ing. Gerda Gläser	69214	gerda.glaeser	Charakterisierung von Solarzellen

Dipl.-Ing. Erik Hoffmann	60106	erik.hoffmann	Laser-induzierte Metallisierung
Irmgard Kerschbaum	67158	irmgard.kerschbaum	Buchhaltung
Lic. Phil. Isabel Kessler	67141	isabel.kessler	Sekretariat, Verwaltung
Dipl.-Ing. Jens Kistner	69223	jens.kistner	Amorphe Solarzellen, Lumineszenz
Dipl.-Pol. Tobias Klaus	69217	tobias.klaus	Öffentlichkeitsarbeit
M. Sc. Gordana Kulushich	69218	gordana.kulushich	Siebdruckprozesse, Modellierung
Dr.-Ing. Jürgen Köhler	67159	juergen.koehler	Laserprozesse, Verwaltung
M. Sc. Patrick Lill	67171	patrick.lill	Laserprozesse
Brigitte Lutz	67200	bigitte.lutz	Analytik, Elektrochemie
Rainer Maak	67158	rainer.maak	Buchhaltung
Dipl.-Ing. Rainer Merz	67184	rainer.merz	Integrierte Photovoltaik

Prof. Dr. Shinsuke Miyajima	67178	shinsuke.miyajima	Dielektrische Passivierschichten
Heike Mohr	67141	heike.mohr	Sekretariat, Verwaltung
M. Sc. Viet Nguyen	67160	viet.nguyen	Siebdruckprozesse, Diffusion
Dipl.-Phys. Kathrin Ohmer	69216	kathrin.ohmer	Laserdotieren
Dipl.-Phys. Liv Prönneke	67180	liv.proenneke	Optik von Solarzellen
Dipl.-Ing. Michael Reuter	67168	michael.reuter	Dünnes, kristallines Silizium
Anton Riß	67214	anton.riss	Werkstatt
Dipl.-Phys. Tobias Röder	69213	tobias.roeder	Laserprozesse
Dipl.-Ing. (FH) Matthias Saueressig	67180	matthias.saueressig	Technologiesupport
Dipl.-Phys. Martin Schneider	67231	martin.schneider	Technologie kristalliner Si-Solarzellen
Dr.-Ing. Markus Schubert	67145	markus.schubert	Stellv. Institutsleiter, amorphes und nanokristallines Silizium

Dipl.-Ing. Fred Schwerdt	69224	fred.schwerdt	Technologiesupport
Dipl.-Ing. Liviu Stoicescu	67245	liviu.stoicescu	Optische Charakterisierung
Dipl.-Ing. Marc Sämann	67142	marc.saemann	Laser-Kristallisation leitfähiger Oxide
Dipl.-Ing. (FH) Sergej Vollmer	67201	sergej.vollmer	Integrierte Serienverschaltung
Prof. Dr. Dr. habil. Jürgen H. Werner	67140	juergen.werner	Institutsleiter, Leitung Forschung, Lehre, Verwaltung
Dipl.-Ing. (FH) Bigitt Winter	67162	birgitt.winter	Technologiesupport, kristalline Si-Technologie
Dipl.-Ing. Thomas Wurster	67246	thomas.wurster	Leistungselektronik
Dr. rer. nat. Renate Zapf-Gottwick	69225	renate-zapf-gottwick	Industrielle Solarzellen
Dr.-Ing. Bastian Zinßer	67170	bastian.zinsser	Erträge von PV-Anlagen

Lageplan

Location Plan

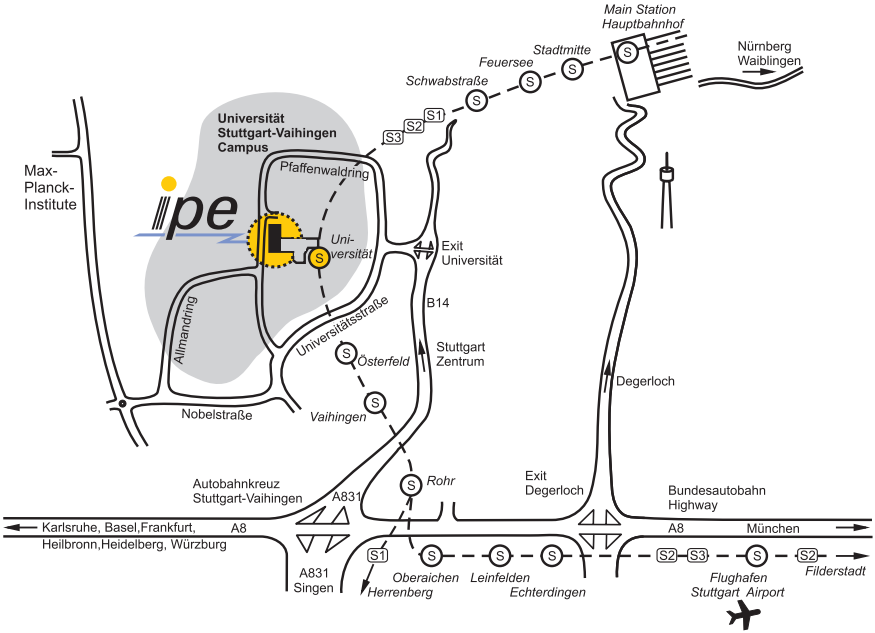

Institut für Physikalische Elektronik
Pfaffenwaldring 47
70569 Stuttgart
Tel.: 0711 / 685-67141

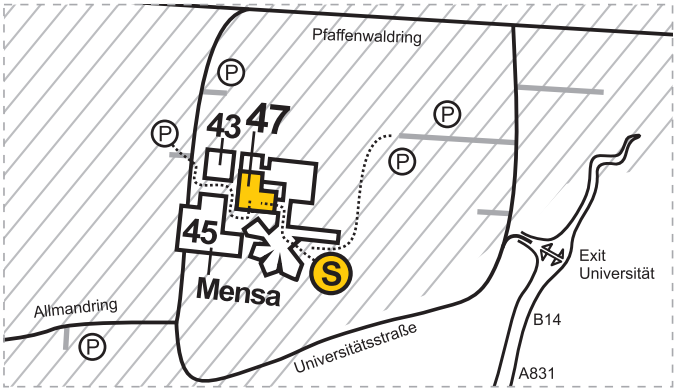

Institut für Physikalische Elektronik
Universität Stuttgart

Pfaffenwaldring 47
70569 Stuttgart

Phone: +49 711 685 67141
FAX: +49 711 685 67143

www.ipe.uni-stuttgart.de